

AD-A169 792

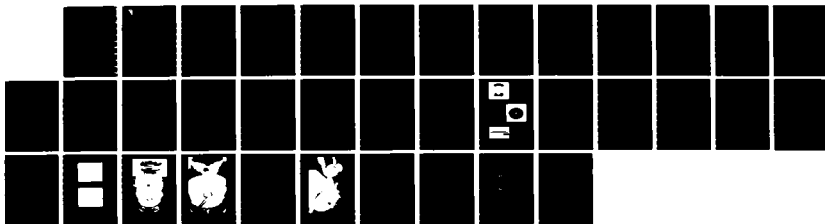
ADVANCED ELECTRIC PROPULSION MPD (MAGNETOPLASMA DYNAMIC)  
(U) PRINCETON UNIV NJ DEPT OF MECHANICAL AND AEROSPACE  
ENGINEERING A J KELLEY ET AL. MAY 86 AFRPL-TR-86-044  
F04611-79-C-0039

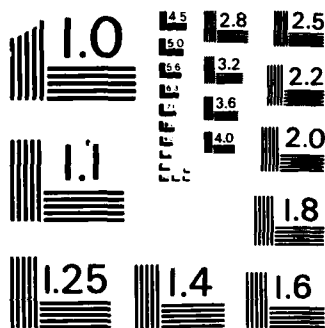
1/1

UNCLASSIFIED

F/G 21/3

NL





MICROCOPY RESOLUTION TEST CHART  
NATIONAL BUREAU OF STANDARDS - 1963 - A



AFRPL TR-86-044

AD:

2

Final Report  
for the period  
15 August 1979 to  
31 May 1986

# Advanced Electric Propulsion MPD

## AD-A169 792

May 1986

Authors:  
A. J. Kelley  
W. Von Jaskowsky  
J. Polk  
R. G. Jahn

Princeton University  
Department of Mechanical and  
Aerospace Engineering  
Princeton, NJ 08544

F04611-79-C-0039

### Approved for Public Release

Distribution is unlimited. The AFRPL Technical Services Office has reviewed this report, and it is releasable to the National Technical Information Service, where it will be available to the general public, including foreign nationals.

*prepared for the:*

**Air Force  
Rocket Propulsion  
Laboratory**

Air Force Space Technology Center  
Space Division, Air Force Systems Command  
Edwards Air Force Base,  
California 93523-5000

DTIC FILE COPY

86 7 14 024

## NOTICE

When U.S. Government drawings, specifications, or other data are used for any purpose other than a definitely related government procurement operation, the government thereby incurs no responsibility nor any obligation whatsoever, and the fact that the government may have formulated, furnished, or in any way supplied the said drawings, specifications, or other data, is not to be regarded by implication or otherwise, or conveying any rights or permission to manufacture, use, or sell any patented invention that may in any way be related thereto.

## FOREWORD

This report was prepared for the Air Force Rocket Propulsion Laboratory (AFRPL) under contract F04611-79-C-0039 by Princeton University. The work was performed during the period 15 August 1979 to 31 May 1986. Principal investigators for Princeton University were A. J. Kelly, W. von Jaskowsky, and R. G. Jahn. Project Manager for the AFRPL was Lt Robert D. Meya.

This technical report has been reviewed and is approved for publication and distribution in accordance with the distribution statement on the cover and on the DD Form 1473.

  
ROBERT D. MEYA, 2LZ, USAF  
Project Manager

FOR THE DIRECTOR

  
EDWARD S. HUSTON, Maj, USAF  
Chief, Space Propulsion Branch

  
CLARK W. HAWK  
Chief, Liquid Rocket Division

## REPORT DOCUMENTATION PAGE

1a. REPORT SECURITY CLASSIFICATION <b>UNCLASSIFIED</b>		1b. RESTRICTIVE MARKINGS	
2a. SECURITY CLASSIFICATION AUTHORITY		3. DISTRIBUTION/AVAILABILITY OF REPORT  <b>Approved for Public Release. Distribution is Unlimited.</b>	
2b. DECLASSIFICATION/DOWNGRADING SCHEDULE		4. PERFORMING ORGANIZATION REPORT NUMBER(S)	
4. PERFORMING ORGANIZATION REPORT NUMBER(S)		5. MONITORING ORGANIZATION REPORT NUMBER(S)  <b>AFRPL-TR-86-044</b>	
6a. NAME OF PERFORMING ORGANIZATION  <b>Princeton University</b>	6b. OFFICE SYMBOL <i>(If applicable)</i>	7a. NAME OF MONITORING ORGANIZATION  <b>Air Force Rocket Propulsion Laboratory</b>	
6c. ADDRESS (City, State and ZIP Code) <b>School of Engineering and Applied Science Princeton, NJ 08544</b>		7b. ADDRESS (City, State and ZIP Code) <b>AFRPL/LKCJ Edwards Air Force Base CA 93523-5000</b>	
8a. NAME OF FUNDING/SPONSORING ORGANIZATION	8b. OFFICE SYMBOL <i>(If applicable)</i>	9. PROCUREMENT INSTRUMENT IDENTIFICATION NUMBER  <b>F04611-79-C-0039</b>	
8c. ADDRESS (City, State and ZIP Code)		10. SOURCE OF FUNDING NOS.	
		PROGRAM ELEMENT NO.	PROJECT NO.
		TASK NO.	WORK UNIT NO.
11. TITLE (Include Security Classification) <b>ADVANCED ELECTRIC PROPULSION MPD (U)</b>		<b>62302F</b>	<b>5730</b>
		<b>05</b>	<b>EQ</b>
12. PERSONAL AUTHOR(S) <b>Kelly, A.J.; von Jaskowsky, W; Polk, J; and Jahn, R.G.</b>			
13a. TYPE OF REPORT <b>Final</b>	13b. TIME COVERED <b>FROM 79/8/15 TO 86/5/31</b>	14. DATE OF REPORT (Yr., Mo., Day) <b>86/5</b>	15. PAGE COUNT <b>35</b>
16. SUPPLEMENTARY NOTATION			
17. COSATI CODES		18. SUBJECT TERMS (Continue on reverse if necessary and identify by block number)	
FIELD	GROUP	SUB. GR.	
<b>21</b>	<b>03</b>	<b>Magnetoplasmadynamic Thruster, Electric Propulsion, Surface Layer Activation Technique.</b>	
19. ABSTRACT (Continue on reverse if necessary and identify by block number)			
<p>An in-situ method of measuring MPD thruster component erosion has been developed and tested on a reference multimegawatt thruster configuration. The technique involves activation of selected areas on the components to be studied by precisely controlled high energy (MeV) ion beam bombardment. Monitoring the decrease in activity during thruster operation provides a precise (sub-micron accuracy), quantitative measure of the amount of material removed from the surface. In preliminary tests, erosion of the tungsten cathode occurred at all operating conditions, but a number of factors contributed to the lack of detectable erosion of the copper anode or the boron nitride insulator. These results tentatively indicate that cathode erosion is linearly related to the charge transfer, but scatter in the individual test sequence erosion rate data prevents a more definitive conclusion to be drawn at this time. Nevertheless, a comparison of erosion data obtained at two different pulse lengths (1 msec, 2 msec) indicates that cathode material loss is generally independent of the number of current transients. Work is continuing in a broad</p>			
20. DISTRIBUTION/AVAILABILITY OF ABSTRACT <b>UNCLASSIFIED/UNLIMITED <input checked="" type="checkbox"/> SAME AS RPT. <input type="checkbox"/> DTIC USERS <input type="checkbox"/></b>		21. ABSTRACT SECURITY CLASSIFICATION  <b>UNCLASSIFIED</b>	
22a. NAME OF RESPONSIBLE INDIVIDUAL  <b>Robert D. Meya, 2Lt, USAF</b>		22b. TELEPHONE NUMBER <i>(Include Area Code)</i> <b>(805) 277-5473</b>	22c. OFFICE SYMBOL  <b>LKCJ</b>

SECURITY CLASSIFICATION OF THIS PAGE

Block 19 (continued):

effort to refine the Surface Layer Activation (SLA) technique and to obtain a data base for additional thrusters.

## TABLE OF CONTENTS

	<u>PAGE</u>
Introduction	1
Experimental Apparatus and Procedure	2
Results and Discussion	4
Thruster Operation	4
Component Erosion	6
Summary	8
Future Research	9
References	10



Accession For	
NTIS GRA&I	<input checked="" type="checkbox"/>
DTIC TAB	<input type="checkbox"/>
Unannounced Justification	
By _____	
Distribution/	
Availability Codes	
Dist	Avail and/or Special
A-1	

## LIST OF FIGURES

<u>FIGURE</u>	<u>TITLE</u>	<u>PAGE</u>
1	Benchmark Thruster	13
2	Vacuum Facility	14
3	Irradiated Components	15
4	Component Spectrum Full Scale Thruster Erosion Test	16
5	Background Striping with a Linear Approximation	17
6	Copper Activity Profile	18
7	Boron Nitride Activity Profile	19
8	Tungsten Activity Profile	20
9	Terminal Characteristics Full Scale Thruster Erosion Test	21
10	Oscilloscope Current and Voltage Traces	22
11	Post-Run Photo of Lucite Insulator	23
12	Post-Run Photo of Cathode	24
13	Voltage Fluctuation Full Scale Thruster Erosion Test	25
14	Post-Run Photo of Anode	26
15	Cathode Erosion vs. Number of Discharges	27
16	Cathode Erosion vs. Charge Transfer	28
17	Half-Scale Flared Anode Thruster	29

## Introduction

High power magnetoplasmadynamic (MPD) thruster current level and longevity are limited by electrode and insulator erosion. As part of a broadly-based effort to assess erosion rates and to understand and to model erosion processes the Electric Propulsion Laboratory at Princeton University is pursuing a program involving development of an in-situ erosion monitoring system, the use of this system to study thruster behavior, and the development of a predictive model of the underlying mechanisms.

Two erosion measurement systems were evaluated during the initial (Phase I) portion of this program<sup>1</sup>. As part of this study boron nitride insulator erosion was measured using flush-mounted quartz crystal microbalances (QCM). The high sensitivity of the microbalance frequency to crystal mass permitted an accurate measure of the sputter-deposited boron nitride surface loss to be obtained. While this method is capable of providing a very accurate measure of surface material loss, its use is limited to low temperature insulator surfaces and therefore lacks general applicability. Nevertheless, the technique is capable of providing believable results. In particular, it was discovered that backplate erosion markedly increases beyond onset and is highest in proximity to the cathode base<sup>2</sup>.

The second technique that was evaluated during the first phase involves the irradiation and transmutation of localized areas (5mm diameter) on the cathode, anode, and insulator to produce a slightly radioactive (<10  $\mu$ Ci activity) surface layer. A depth/activity calibration curve obtained from an identically irradiated and prepared test sample permits changes in activity to be accurately interpreted in terms of surface material loss. It is this surface layer activation (SLA) method that was selected for further development. Not only does the SLA technique provide the requisite submicron level accuracy but, most importantly, it has wide applicability<sup>3</sup>, to a broad array of materials and demanding operating conditions.

This report provides a general summary of the SLA erosion monitoring method. In addition, the results that have been obtained by application of the technique to the measurement of erosion behavior of multimegawatt MPD thruster components are also presented. These test results have permitted tentative

conclusions concerning general surface loss mechanisms to be drawn.

In the interests of clarity and conciseness, details of the work have been omitted. A comprehensive archival literature base exists for this work in the form of monthly technical progress reports which are available from the Princeton University Engineering Library. These reports have been bound into yearly compendia which can be obtained by requesting: MAE Report #1672 for 1979, MAE Report #1673 for 1980, MAE Report #1674 for 1981, MAE Report #1675 for 1982, MAE Report #1676 for 1983 and MAE 1677 for 1984. Alternatively, individual monthly reports relating to specific topics can be obtained directly from A.J. Kelly.

#### Experimental Apparatus and Procedure

The reference or "full-scale" coaxial thruster configuration shown in Figure 1 was used for all tests in this study. This configuration was chosen for several reasons. Not only is there a large experimental data base for this design, but, of equal importance, the QCM measurements of insulator erosion<sup>2</sup> were performed with this geometry. Consequently, a basis for direct comparison of the two measurement techniques is available.

As depicted in the figure, a 10 cm long by 1.9 cm diameter thoriated tungsten cathode, mounted on the centerline of the thruster, is separated from the 18.7 cm outer diameter, 10.2 cm inner diameter copper anode by boron nitride and lucite insulators which form the backplate and sidewalls of the 12.7 cm diameter by 5.1 cm deep thrust chamber. Argon propellant, injected through a high speed solenoid valve, is distributed by an annulus in the boron-nitride backplate surrounding the cathode and enters the interelectrode zone via twelve equispaced 3mm holes circularly arrayed at a radius of 3.8 cm.

The thruster assembly, mounted for test in a fiberglass vacuum tank 1.8 m in diameter and 4.8 m long, as shown in Figure 2, experiences prerun pressures of about  $10^{-5}$  torr. The arc current is provided by a 3000  $\mu$ F pulse forming network producing up to 30 kiloamperes in 1 msec rectangular pulses or up to 15 kiloamps in 2 msec pulses.

As indicated in Figure 1 and the photos of Figure 3, one 0.5 cm diameter "spot" on the tungsten cathode, copper anode, and boron nitride backplate was activated by bombardment with a high energy alpha or proton beam. The cathode and backplate spot positions were chosen on the basis of spectroscopic data and the QCM experiment results which showed erosion to be most severe in these regions, that is, at the base of the cathode and close to the cathode on the backplate. The anode was irradiated on the downstream plane face radially outward and in the proximity to the lip radius.

The isotope and beam parameters used for these tests are shown in Table 1. Isotope selection is based on a number of considerations, all of which have had to be addressed to obtain meaningful results. Target surface disruption is limited by selecting the beam energy that corresponds to the maximum collision cross-section for the desired transmutation irradiation. Beam energy also determines the depth of penetration and therefore the activity depth profile, with overall activity level being determined by the total charge transfer. In addition, the specific isotopes to be used are chosen to have half-lives which are sufficiently long to permit an adequate time for testing. Over and above these considerations, the activated depth must be capable of providing a detectable erosion-related change after a reasonable number of shots (<1000). Added to all of this is the requirement that the resultant gamma ray spectrum be well defined and distinct from others used in the experiment. Finally, the activity levels were chosen to provide a strong gamma signal consistent with nuclear safety regulations and the desire to involve an absolute minimum of irradiated material in the experiment. With effort all of these disparate factors can be simultaneously satisfied as is evidenced by the spectrum of Figure 4 where the distinct, well separated photopeaks produced by the three isotopes  $Os^{185}$  (tungsten),  $Zn^{65}$  (copper), and  $Be^7$  (boron nitride), are displayed.

The gamma radiation produced by the irradiated spots is only slightly attenuated by the surrounding thruster body. Consequently, a 5" by 5" NaI (Tl) scintillator crystal mounted in juxtaposition to the thruster can detect these emissions and provide a low noise output that is approximately proportional to the gamma ray energy. Once collected by a multi-channel analyzer the spectra

are analyzed. The background radiation from each of the three photopeaks is automatically subtracted by using a linear approximation involving the fitting of a line to four points at each end of the particular range of interest, as is illustrated in Figure 5. The countrate is then determined from the collection time and the counts in each photopeak. This countrate, when normalized by the pre-firing count-rate and corrected for natural decay, is a direct measure of the existing material activity level.

The eroded depth is determined by comparing this normalized activity level with the previously generated activity-depth profile curves. These depth profiles are obtained by first irradiating copper, tungsten, and boron nitride samples formed from the same materials and handled in precisely the same manner as the thruster components. Precision lapping of the surfaces then permits an accurate depth-activity profile to be developed. Profiles for the three materials are shown in Figures 6-8, where the '+'s are from samples irradiated to about 1.5 microcuries and the '\*'s are from samples irradiated to about twice that level. The profiles are seen to be independent of the intensity of the activity and can be used with confidence to measure mass loss from similar materials providing the test item is irradiated in accordance with the conditions noted in Table 1.

A mass flow rate of three grams per second was used throughout all of the individual test sequences noted in Table 2. All told, the thruster testing involved some 24,420 discharges representing a total charge transfer of 461,975 Coulombs. Four current levels -- 10, 15, 23, and 27 kiloamperes -- were examined, with particular emphasis being placed on the 23 kiloamperes discharges, which should have been near or above the thruster onset current. A pulse length of 1 msec was used for all except one test sequence in which 2 msec pulses at 15 kiloamps were used to evaluate the influence of start/stop transients on erosion.

## Results and Discussion

### Thruster Operation

The test thruster terminal voltage current characteristic data are summarized in Figure 9. For comparison purposes the results obtained from a

similar thruster<sup>4</sup> studied by Kaplan are also displayed in this figure. The general scatter and the overall behavioral pattern of these data, each point of which represents the mean voltage of a number of shots at fixed voltage, reflect the operational peculiarities of this device. The clearly defined divergence that exists between the two data sets at high current indicates that additional mass, over and above the nominal injected mass flow rate, was present during the erosion tests.

In addition, a number of the 15 kA, voltage traces exhibited an unusual stepped behavior. During normal operation, the voltage starts at some high value, drops to a quasi-steady value during breakdown, remains at this level until the end of the current pulse, whereupon it decays rapidly to zero, cf. Figure 10. In contrast to this, for the first two test run sequence at 15 kA, approximately 40% of the voltage traces were similar to the one shown in Figure 10, where the voltage steps up to a second quasi-steady level in the middle of the current pulse. In the final run sequence at 15 kA, approximately 70% of the traces were of this form. The voltage mean of the lower half of the stepped traces is plotted as squares in Figure 9 and the upper plateau voltages are displayed as triangles. As can be noted, the observed voltages for the first half of the current pulse correspond more closely with previous test data than do those of the latter portion. It is doubtful that this can be attributed to additional mass flow into the thruster, but more likely is due to a transition from one mode of arc behavior to another, such as from a diffuse discharge to a spoked discharge attaching preferentially in one location.

Post-test inspection of the thruster revealed that indeed there was an additional source of mass present, lending credence to the inference from the terminal voltage characteristics. The lucite insulator that formed the sidewalls of the thrust chamber was found to be heavily eroded (cf Figure 11). Moreover, as displayed in Figure 12, adjacent portions of the cathode were coated with a heavy (~0.5 mm thick) carbonaceous layer presumably formed by condensation of lucite decomposition products.

Inspection of the lucite sidewall revealed that approximation 8 mL of the methylacrylate were ablated. If this material was uniformly ablated over the

course of the 24,420 discharges of the test program, the flow of ablation products would have added about 1 g/s to the nominal 3 g/s of argon propellant flowrate. Further, if full dissociation of the relatively low molecular weight ablated material is assumed, the corresponding number density of the lucite and argon would have been quite similar. It must be concluded that the true mass flow rate and propellant composition for the test sequence are uncertain and could have fluctuated within broad limits during the experiment.

#### Component Erosion

Although cathode erosion was measured at all current levels, no decrease in activity due to erosion was observed in the irradiated spots on the copper anode or on the boron nitride backplate. This contrasts with earlier QCM experiments which showed significant insulator ablation during operation above the onset current. These measurements indicated that for this thruster configuration onset occurs at about 22 kA during operation at 3 g/sec. Consequently, the tests at current levels above 22 kA should have produced detectable erosion of the boron nitride. As indicated by the data of Figure 13, which shows wide fluctuations in the current at which the 10% hash, onset condition was measured, it is difficult to confirm whether any of the test points were actually above onset. The additional mass from the lucite insulator ablation probably has raised the onset current to a level beyond the maximum test currents used. In addition, the depth calibration curve for boron nitride displayed in Figure 7 indicates a relative insensitivity of activity level with depth for approximately the first 10 microns. Therefore, although there were no measurable indications of gross insulator ablation, there may well have been some erosion present and masked by the insensitivity of the technique in this regime. It must be concluded that the combination of operating condition variability and depth calibration insensitivity conspire to limit the results of this analysis to the general statement that it is not inconsistent with previous QCM observations.

The failure to measure erosion of the copper anode is more surprising. Not only did post run visual inspection of the anode show heavy arc attachment damage to the radius of the anode lip, clearly visible in Figure 14, but a comparison of the copper and tungsten depth calibration curves of Figures 6 and 8

shows them to have a comparably high sensitivity. Consequently, the erosive loss of submicron amounts of material from the activated spot would have produced detectable changes in the activity level. This permits the unambiguous conclusion that no mass removal occurred from the activated spot position. A possible explanation for this is that the highest current concentration occurs on the lip radius and not on the face. This conjecture is supported by previous current mapping of a similar anode structure<sup>6</sup> which shows that the activated spot is indeed located in a region of lower current density than is present on the adjacent lip position.

The fact that cathode erosion is present at all current levels indicates that removal of cathode material is an inherent feature of MPD thruster operation consistent with Ho's spectroscopic observations<sup>6</sup>. The plots of cathode erosion as a function of the total number of discharges, Figure 15, and as a function of the charge transfer in Figure 16, indicate a roughly linear relationship between the eroded depth and number of discharges or charge transfer. However, variations of erosion rate with current among the nine level are obviously present. Linear fits to the entire set of data from the nine tests gives these relationships for the erosion rate:

$$E_r = 0.582 \mu/10^3 \text{ discharges}$$

$$E_r = 3.33 \mu/10^5 \text{ C}$$

If the erosion is assumed to be uniform over the cathode surface, the mass loss rate would correspond to an erosion rate of 4.43  $\mu\text{g/C}$ , a rate which is in good agreement with Kuriki's measurements<sup>7</sup>. The data points for each of the nine test sets produced very good linear fits, which are listed as erosion rates in columns (6) and (7) of Table 2. Comparison of these nine data correlations permits several important observations to be made. First, the erosion rates calculated from the different test sequences at 15 and 23 kA are widely scattered, masking any relationship between eroded depth and current level. Interestingly the close linear fit apparent within each of the nine data sets argues against interpreting this scatter in terms of shot to shot mass flow fluctuations. These factors notwithstanding, there is now clear evidence for

cathode erosion being controlled by current flow without a minimum threshold.

Secondly, the data obtained at 15 and 23 kA indicate that the erosion rate decreases with eroded depth. One possible explanation for this relates to the variation in material properties with depth due to radiation damage sustained during activation of the spot. This factor will be studied as a part of our future work. Finally, comparison of the data sets obtained at 15 kA with different current pulse lengths shows an erosion rate for the 2 msec run approximately twice that of the 1 msec runs. This provides, albeit tentative, first evidence that the erosion rate may be more closely dependent on charge transfer than on the number of start-up or decay transients.

#### Summary

Localized areas on the copper anode, tungsten cathode, and boron nitride insulator of an MPD thruster were irradiated to produce a low level of nuclear activity. The activity of these regions permits a direct, quantitative measurement of surface material loss. The eroded depth was related to the observed decrease in activity by using previously measured profiles of normalized activity versus depth. Measurement of these depth profiles for the thruster materials at two different activity levels demonstrates that these profiles are independent of activity level.

Operation of the thruster for 24,420 discharges at different current levels and current pulse lengths produced no significant anode or insulator erosion. Although the anode was visibly eroded on the lip, the face of the anode where the activated spot was located did not ablate. The insulator probably remained undamaged because additional mass from ablation of a lucite sidewall prevented operation above the onset current where heavy insulator erosion is typical. In addition, insensitivity of the method to eroded depths less than ten microns may have masked some erosion.

Cathode erosion was found at all current levels, indicating that this is an inherent feature of MPD operation. Erosion is linearly related to the charge transfer, and occurs at a rate of  $4.43 \mu\text{g}/\text{C}$ , under the assumption of uniform erosion over the cathode surface. Variation of erosion rate with current level was observed, but the data were scattered. This scatter may have been due to

fluctuations in the mass flow rate caused by either lucite sidewall ablation or to changes in material properties with depth due to radiation damage. A test sequence at 15 kA with two different pulse lengths indicates that the erosion rate is relatively insensitive to the number of start-ups and decay transients. These data represent the first in situ quantitative measurement of multimegawatt MPD thruster component erosion and serve as a detailed guide to further research.

#### Future Research

The flared anode thruster configuration shown in Figure 13 will be tested using the SLA technique with activated spots in the indicated positions. This design is a half-scale version of a thruster tested recently at Princeton. The planned test sequence involves continued variation of current level and mass flow in an attempt to explain the scatter of erosion rate with current observed with the full-scale reference thruster. In addition, use of refractory materials in the mass injection system will permit operation of this thruster at a higher pulse rate than has been heretofore possible. This will allow investigation of the effect of higher steady state temperatures on erosion rate. Operation of this half-scale thruster at mass flow rates will make it possible to explore the post onset current region in some depth, where evidence of insulator ablation should be manifest. Irradiation of a spot on the copper anode corresponding to the point of maximum current attachment should also make anode erosion detectable. Simultaneous diagnostic probing of an identical thruster mounted in another test facility will provide information on interelectrode current profiles at different operating conditions, and permit correlation with the erosion data. The effect of radiation damage on the mechanical properties of the irradiated spots will also be investigated in a continuing effort to determine the validity of the Surface Layer Activation technique.

## REFERENCES

1. Clark, K.E. and Jahn, R.G., "Magnetoplasmadynamic (MPD) Thruster Erosion Studies - Phase I", AF Contract No. F04611-79-C-0039, April 1983.
2. Rowe, R., von Jaskowsky, W.F., Clark, K.E., and Jahn, R.G., "Erosion Measurements on Quasi-Steady MPD Thrusters," AIAA Paper 81-0687, April 1981.
3. Marks, L.M., Clark, K.E., von Jaskowsky, W.F., and Jahn, R.F., "MPD Thruster Erosion Measurement," AIAA Paper 82-1884, November 1982.
4. Kaplan, D.I. and Jahn, R.G., "Performance Characteristics of Geometrically Scaled Magnetoplasmadynamic (MPD) Thrusters," Mechanical and Aerospace Engineering Report 1492, Princeton University, Princeton, NJ, February 1982.
5. Rudolph, L.R. and Jahn, R.G., "The MPD Thruster Onset Current Performance Limitation," Mechanical and Aerospace Engineering Report 1491, Princeton University, Princeton, NJ, September 1980.
6. Ho, D.D. and Jahn, R.G., "Erosion Studies in an MPD Thruster," Mechanical and Aerospace Engineering Report 1515, Princeton University, Princeton, NJ, May 1981.
7. Mori, K., Kurikaka, H., Kuriki, I., "Effect of Electrode Configuration on MPD Arcjet Performance," IEPC Paper 84-11, July 1984.

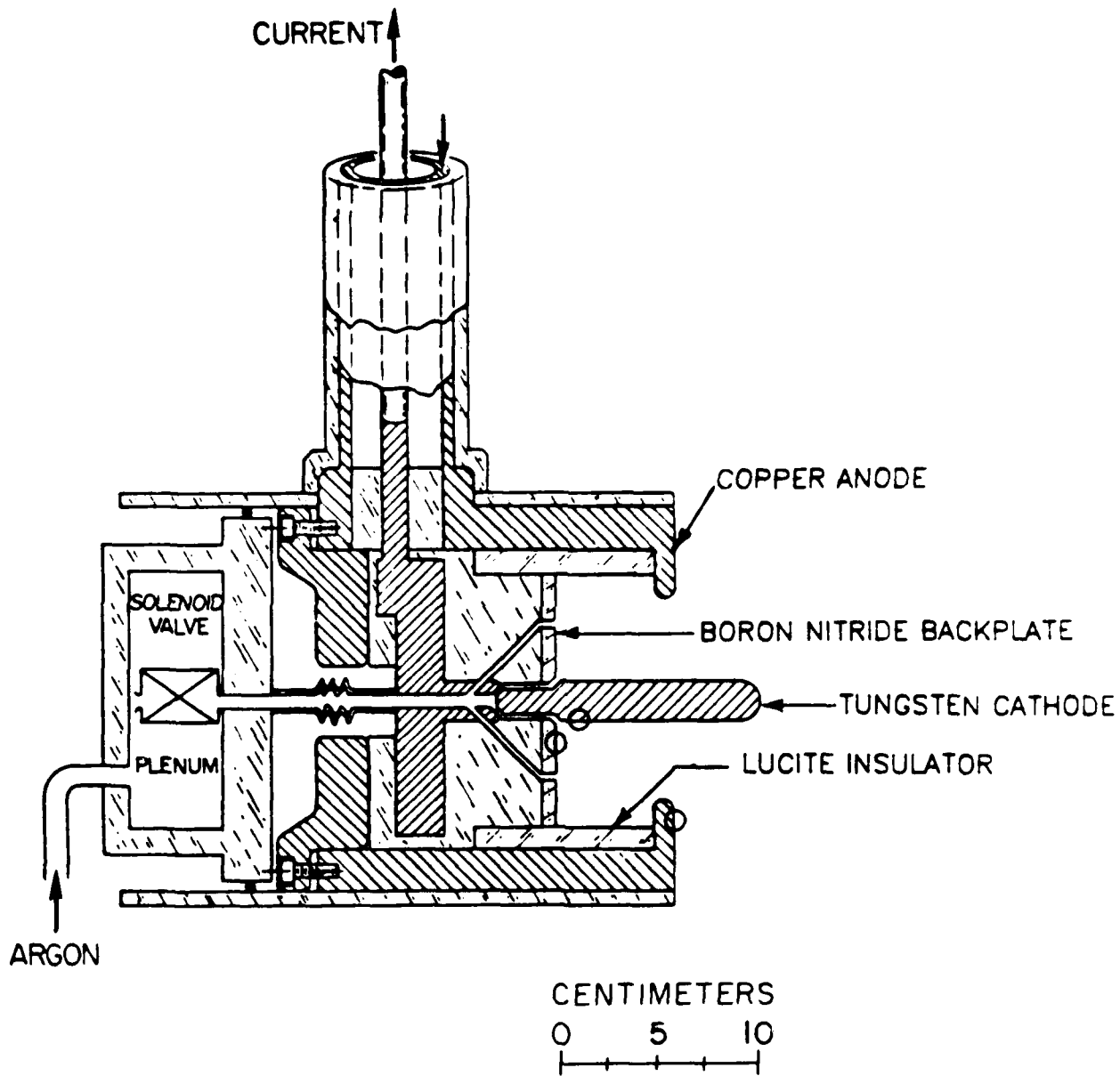
TABLE 1  
ACTIVATION PARAMETERS

	TARGET		
	W	Cu	BN
Isotope	Os <sup>185</sup>	Zn <sup>65</sup>	Be <sup>7</sup>
Beam Energy	26 MeV Alphas	4.92 MeV Protons	4.92 MeV Protons
On Target Beam Energy	23 MeV Alphas	4.25 MeV Protons	2.4 MeV Protons
Aluminum Degraded Thickness	≈2.2 Mil	≈1.3 Mil	≈5.1 Mil
Total Charge on Target	30.67 mC	57.35 mC	22.25 mC
Activity Level (of above isotope)	1.41μ Ci	1.50μ Ci	0.74μ Ci
Production Rate	0.046 μCi/mC	0.026 μCi/mC	0.033 μCi/mC

TABLE 2

TEST SEQUENCE AND CATHODE EROSION DATA SUMMARY  
ORDERED BY CURRENT AND DEPTH RANGE

Run#	Discharges	Current (ka)	Pulse Length (msec)	Depth Range ( $\mu\text{m}$ )	Erosion Rate ( $\mu\text{m}/1000$ discharges)	Erosion Rate ( $\mu\text{m}/10^4$ Coulombs)
7	4656	10	1	10.03-11.91	0.39	3.9
4	975	15	2	5.33-7.04	1.7	5.7
6	2849	15	1	8.27-10.03	0.68	4.4
8	3954	15	1	11.91-13.97	0.52	3.4
1	2478	23	1	1.10-3.12	1.0	4.5
3	620	23	1	4.42-5.33	1.5	6.4
5	2433	23	1	7.04-8.27	0.41	2.0
9	3832	23	1	13.97-15.20	0.34	1.5
2	2623	27	1	3.12-4.42	0.5	1.9



○ - IRRADIATED POSITIONS

FIGURE 1: BENCHMARK THRUSTER

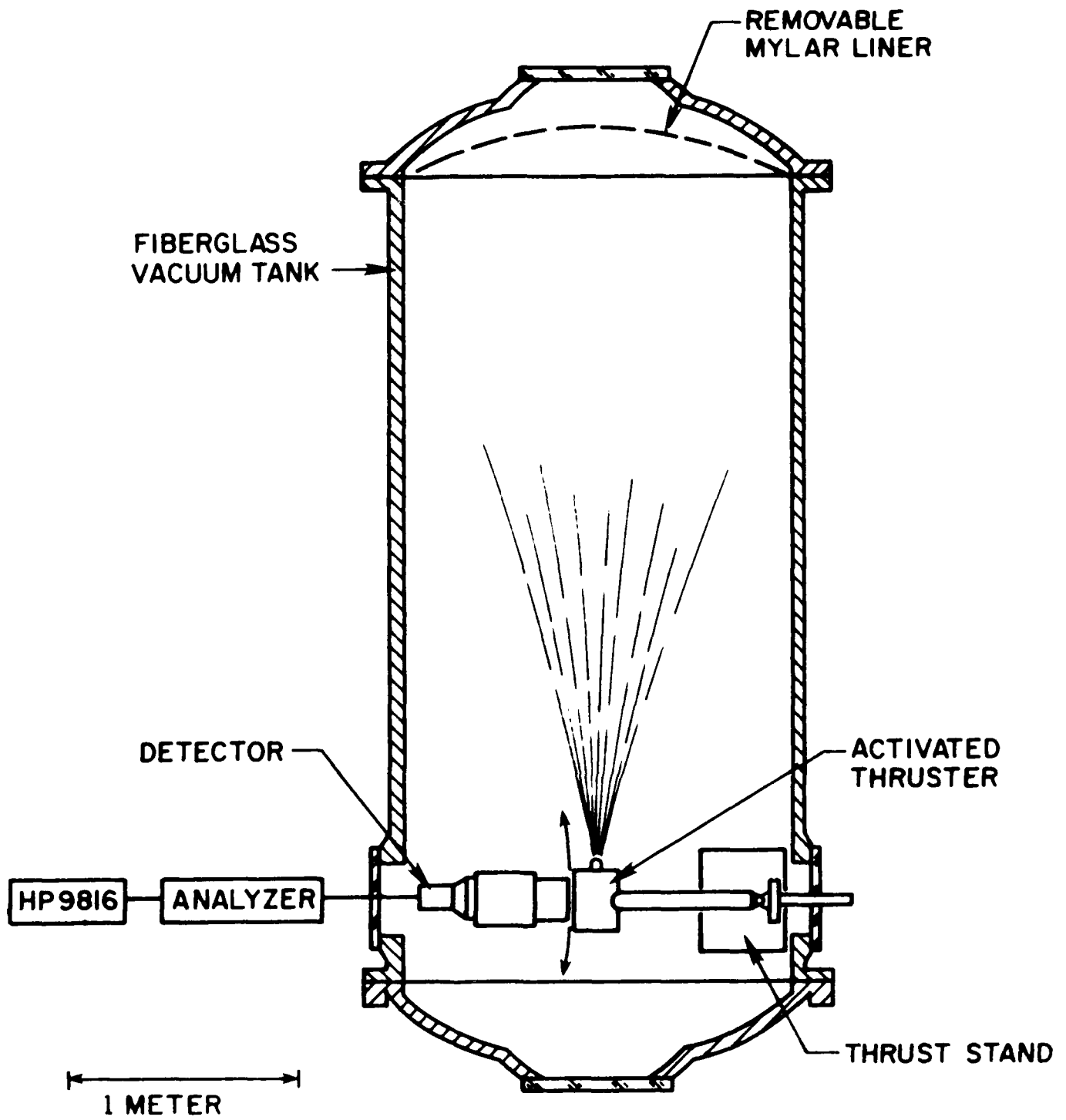
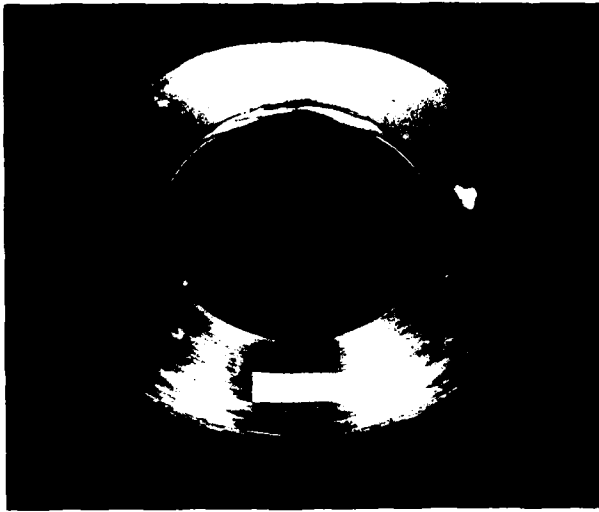
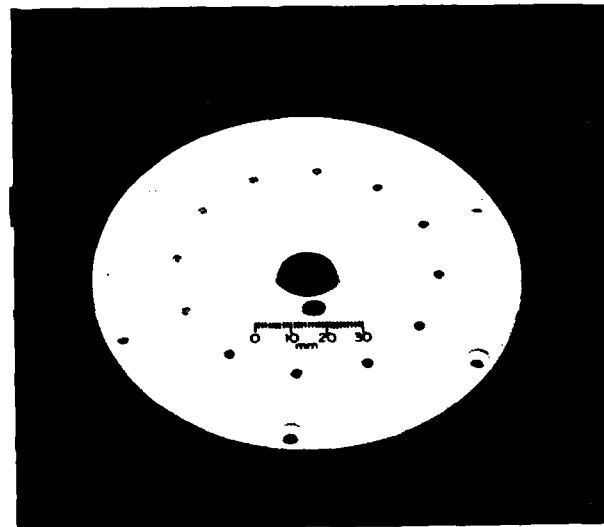


FIGURE 2: VACUUM FACILITY



IRRADIATED COPPER ANODE

IRRADIATED BORON NITRIDE  
BACKPLATE



IRRADIATED TUNGSTEN CATHODE

FIGURE 3: IRRADIATED COMPONENTS

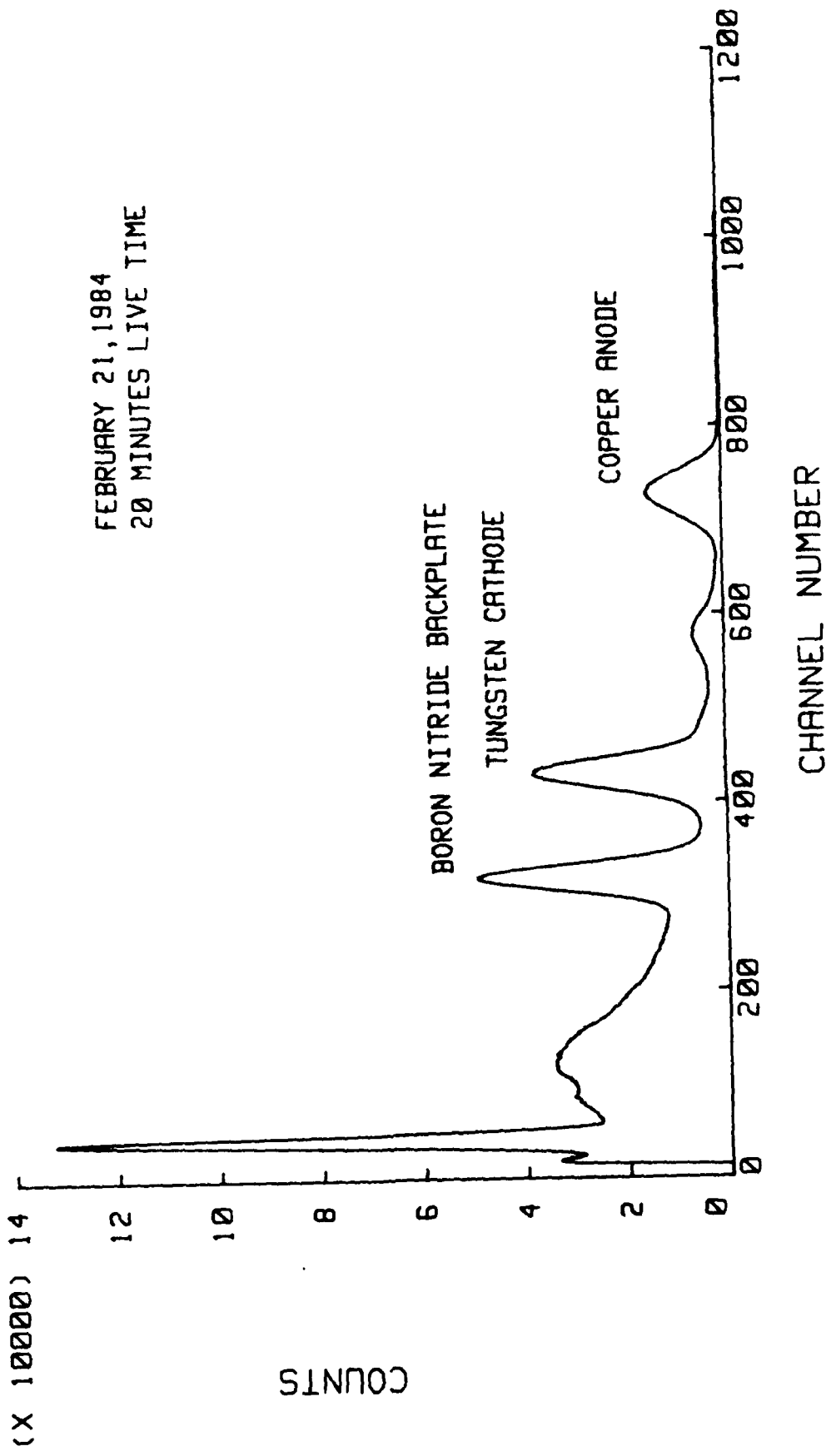


FIGURE 4: COMPONENT SPECTRUM  
FULL SCALE THRUSTER EROSION TEST

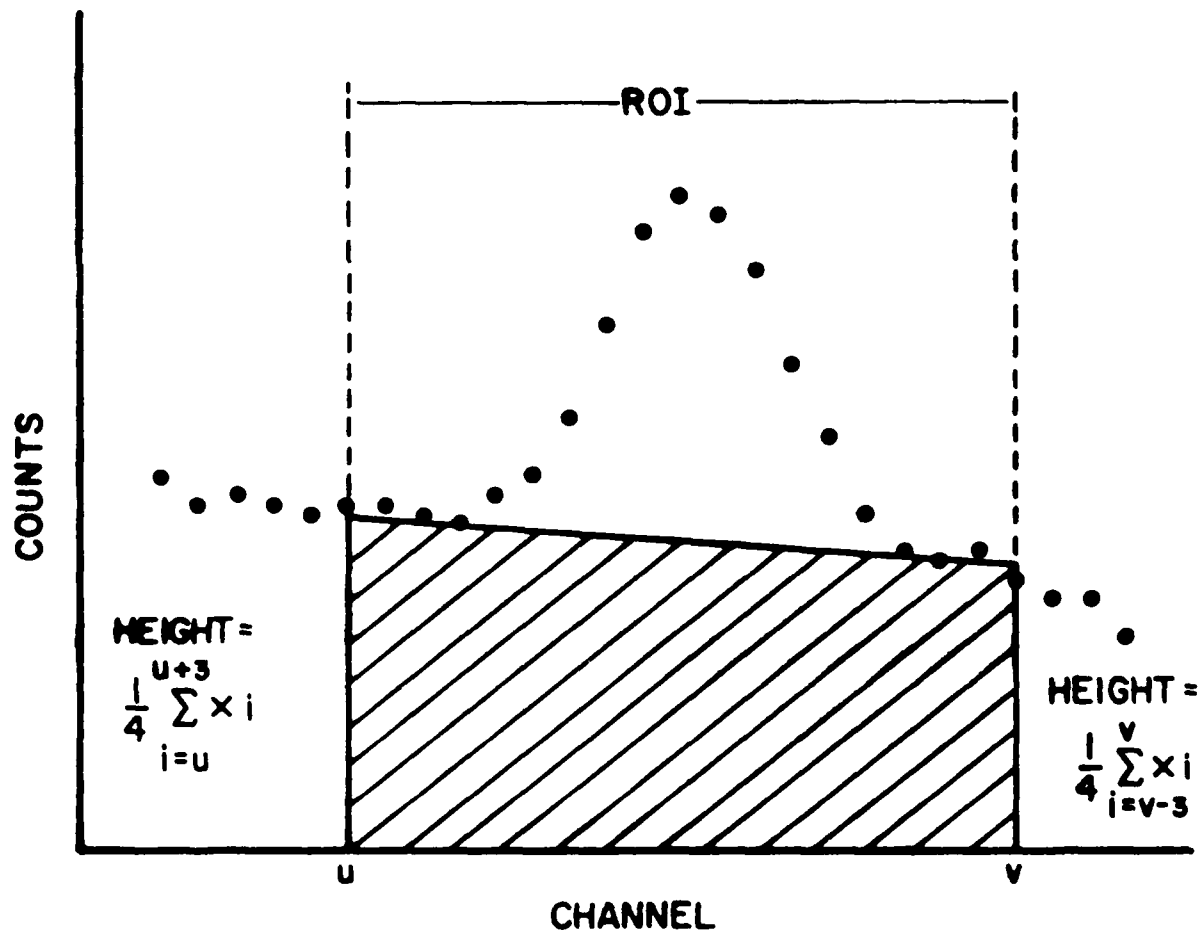


FIGURE 5: BACKGROUND STRIPPING  
WITH A LINEAR APPROXIMATION

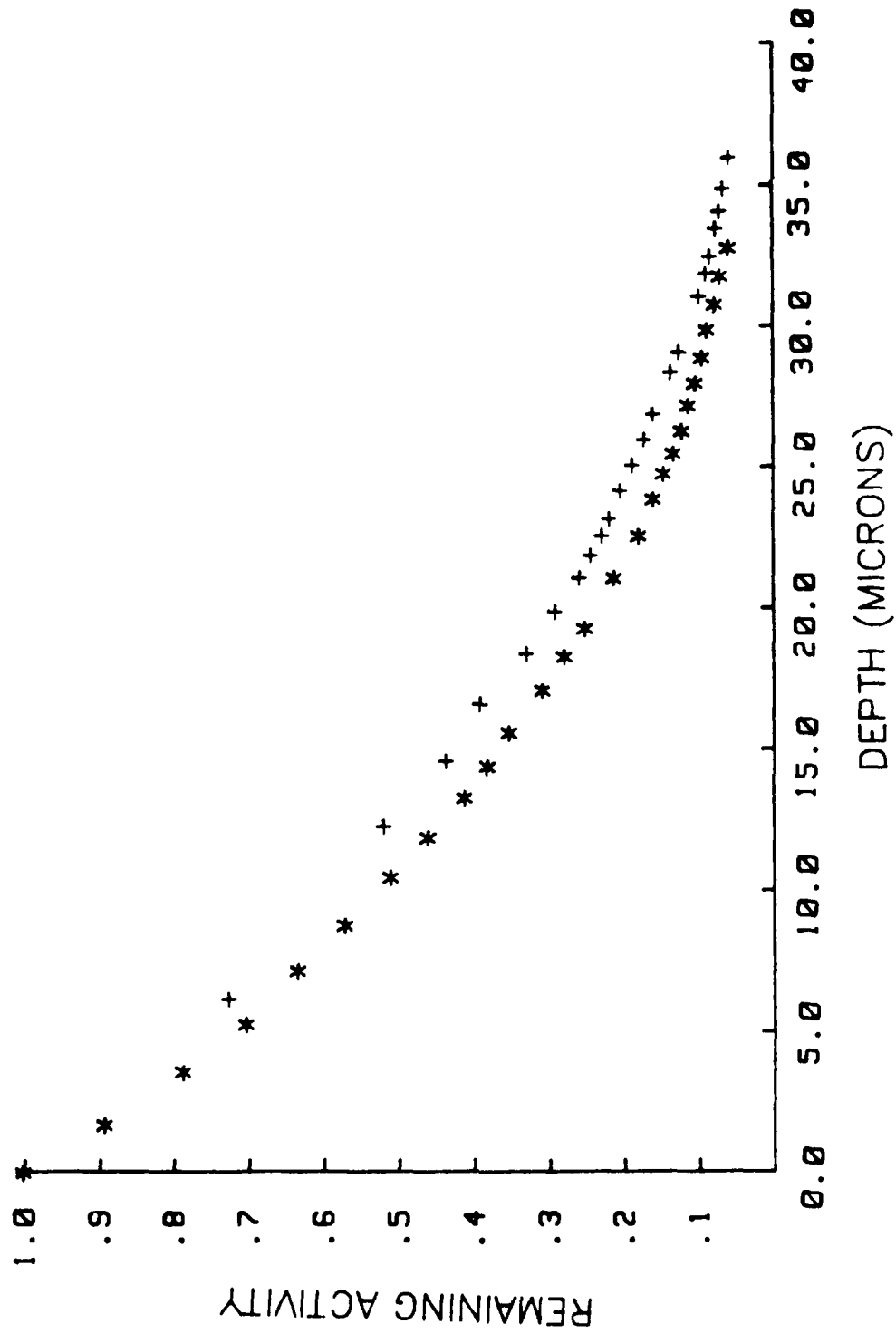


FIGURE 6: COPPER ACTIVITY PROFILE

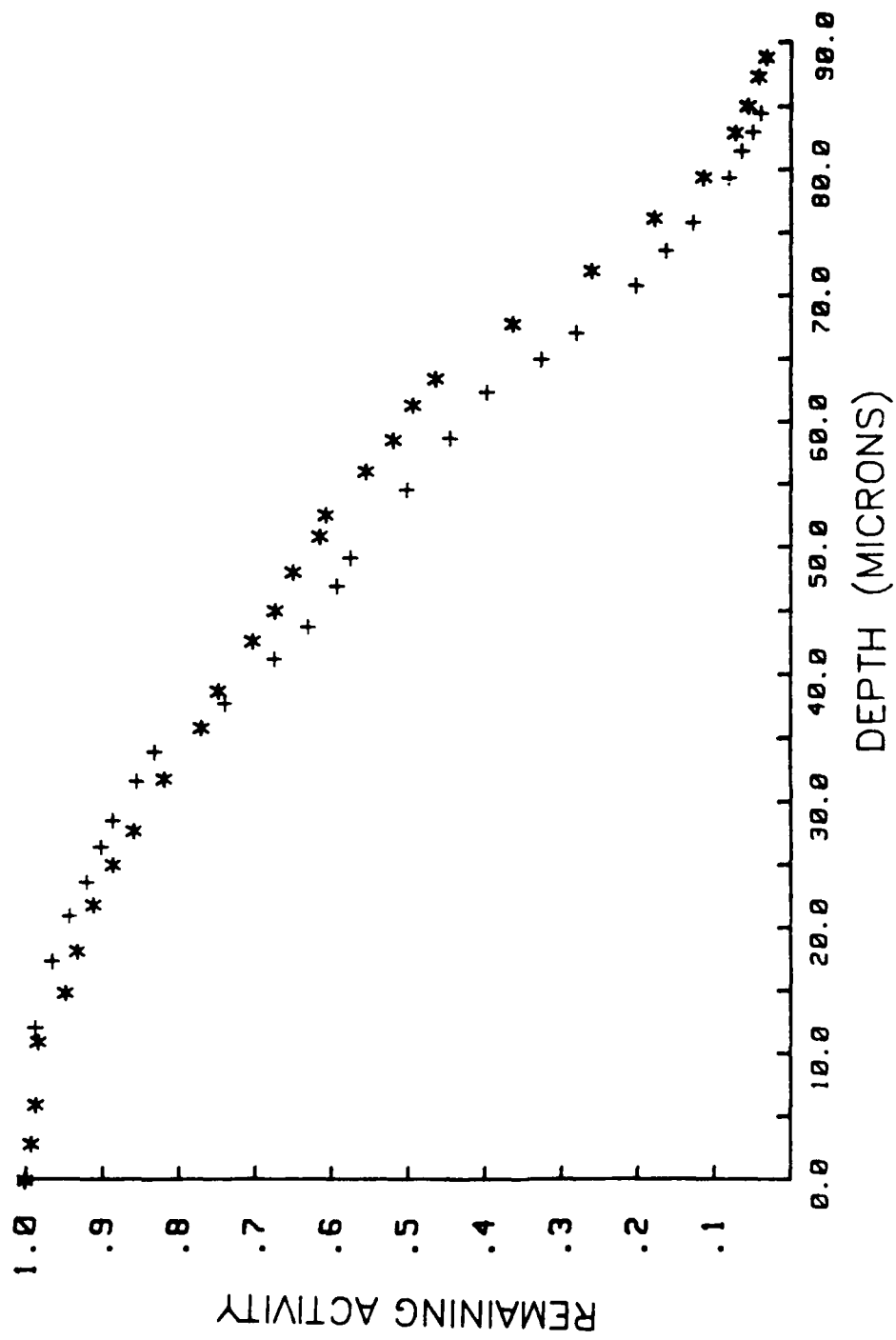


FIGURE 7: BORON NITRIDE ACTIVITY PROFILE

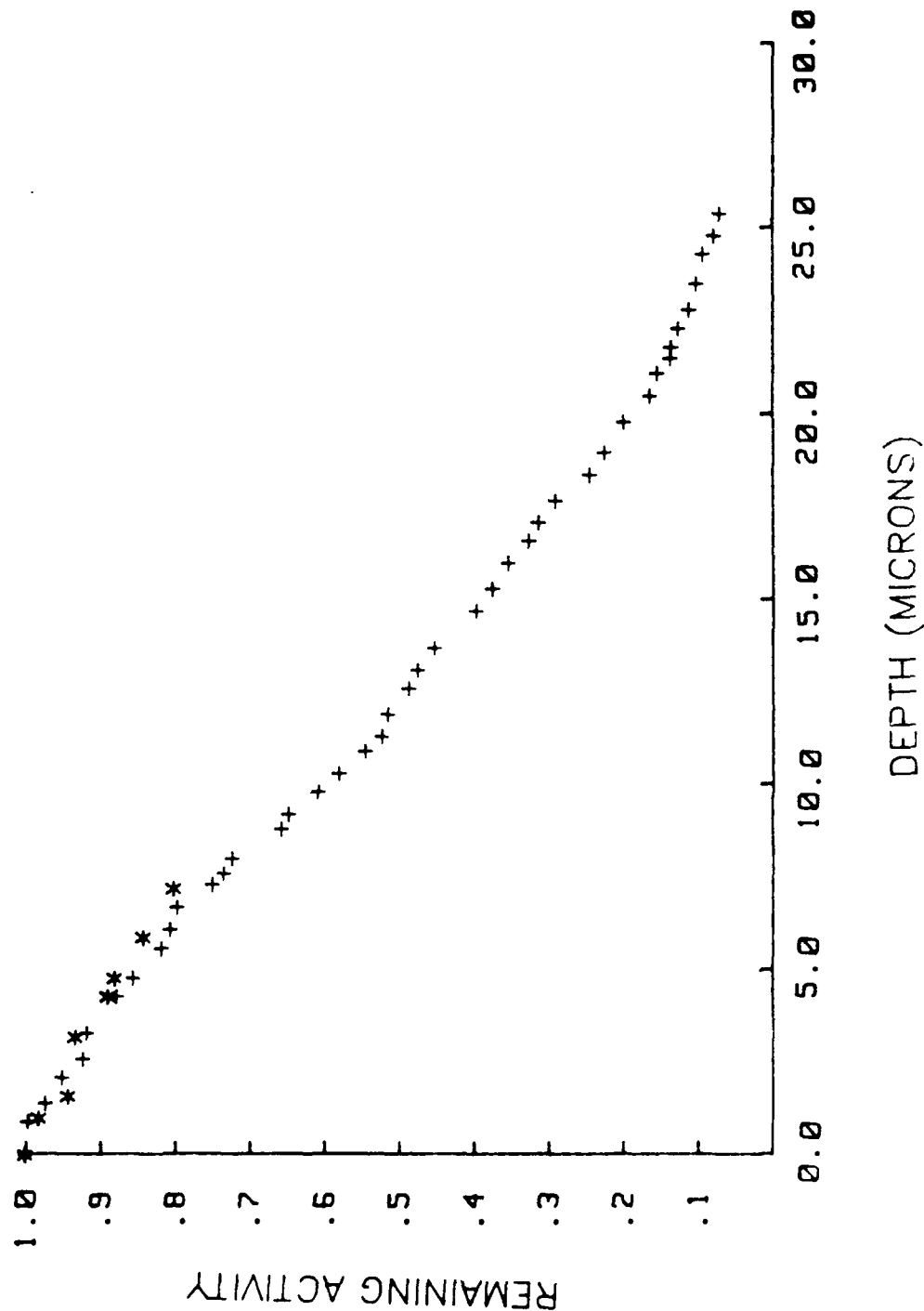
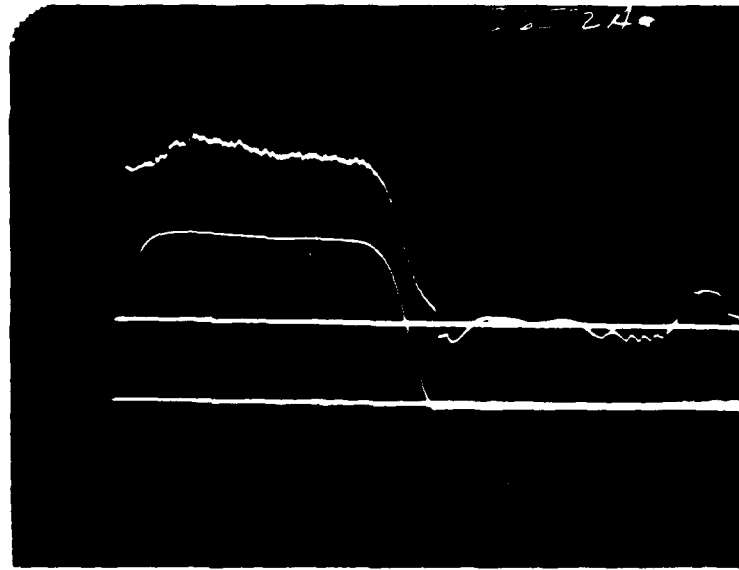


FIGURE 8: TUNGSTEN ACTIVITY PROFILE



TYPICAL VOLTAGE TRACE



IRREGULAR "STEPPED" VOLTAGE TRACE

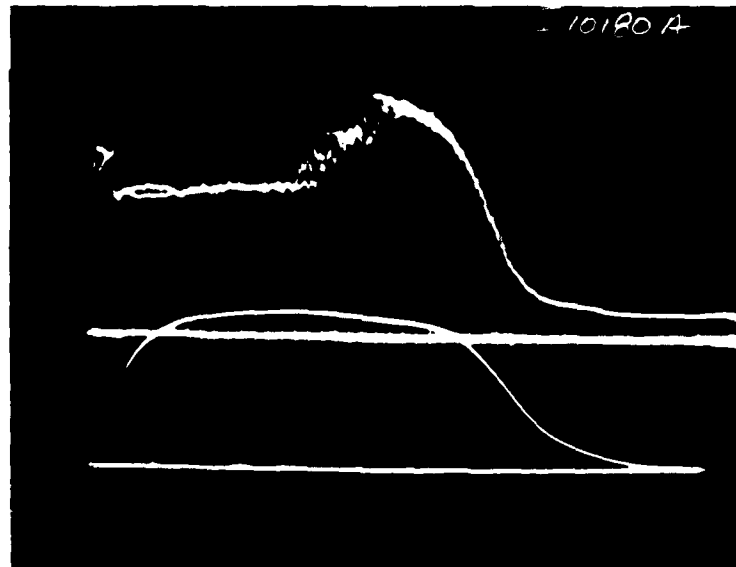


FIGURE 10: OSCILLOSCOPE CURRENT AND VOLTAGE TRACES

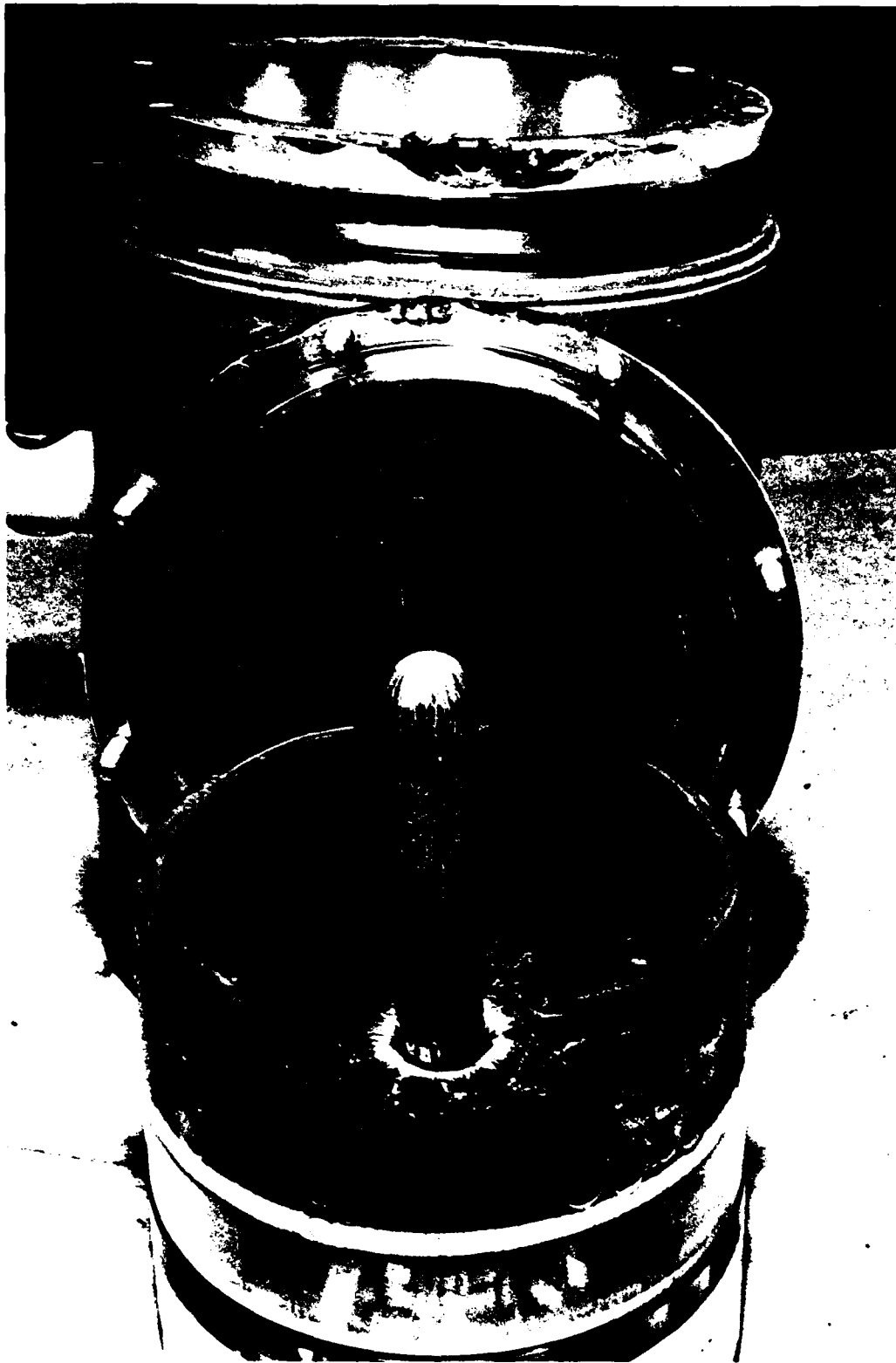


FIGURE 11: POST-RUN PHOTO OF LUCITE INSULATOR



FIGURE 12: POST-RUN PHOTO OF CATHODE





FIGURE 14 : POST-RUN PHOTO OF ANODE

FIGURE 15: CATHODE EROSION VS  
NUMBER OF DISCHARGES

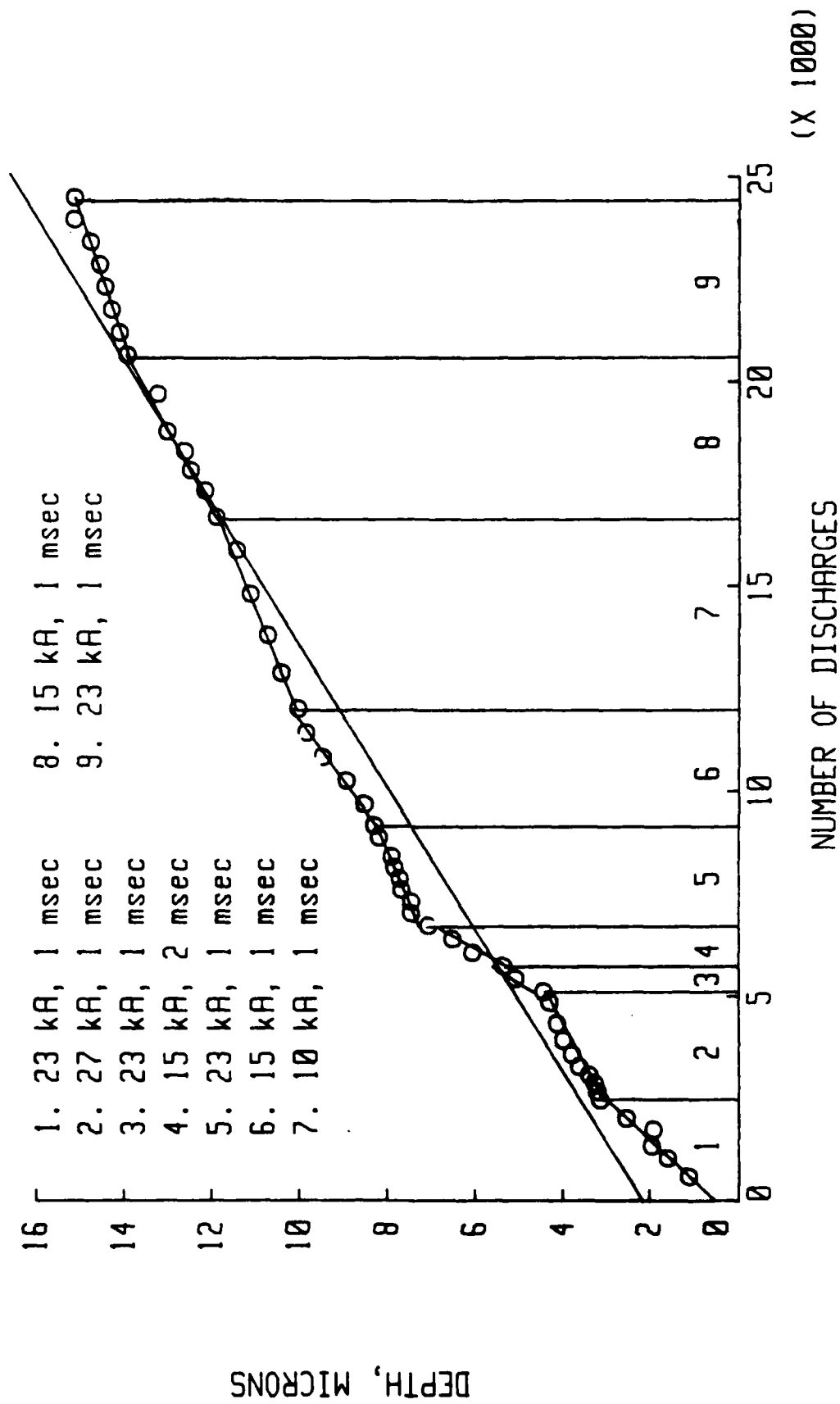


FIGURE 15: CATHODE EROSION VS  
NUMBER OF DISCHARGES

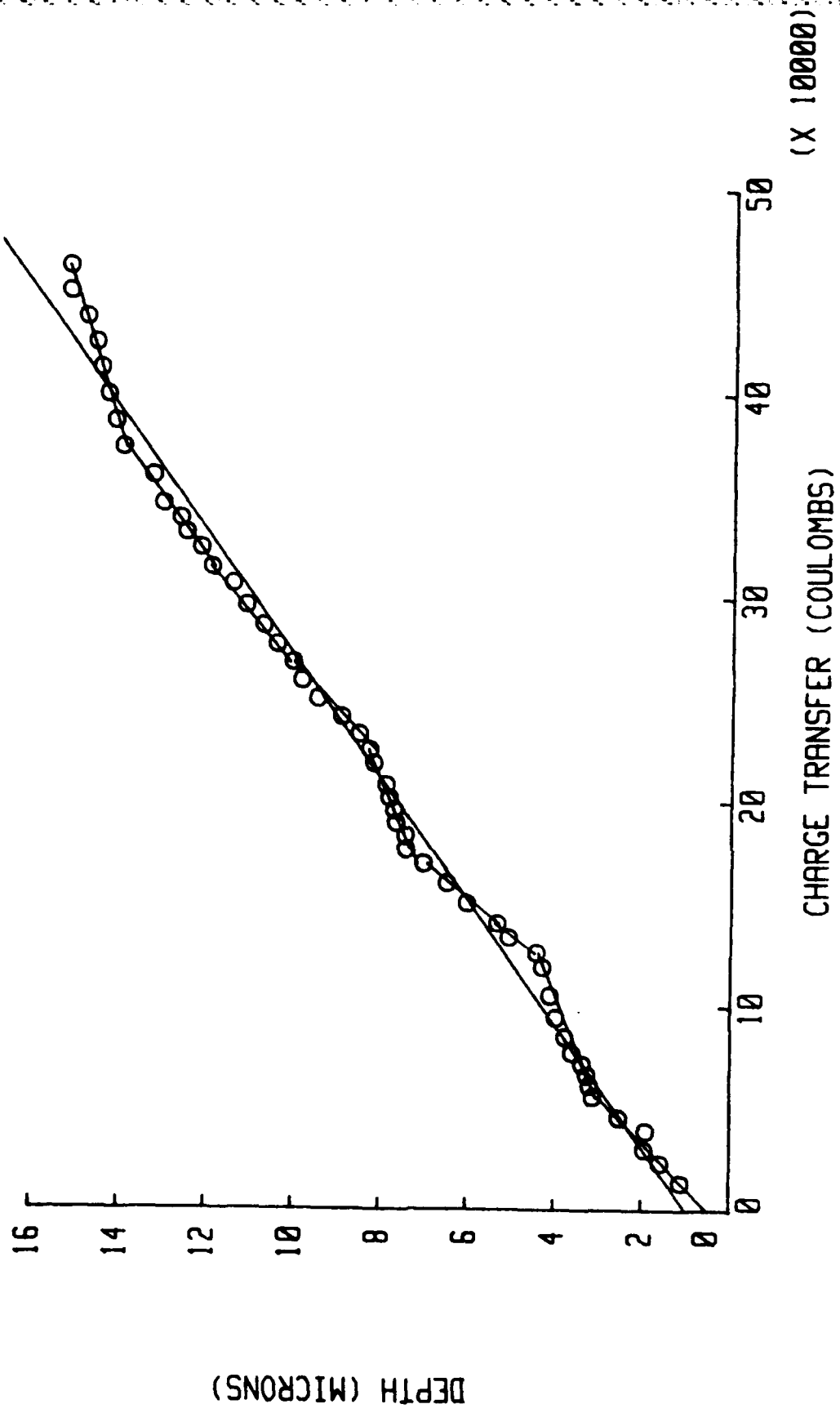
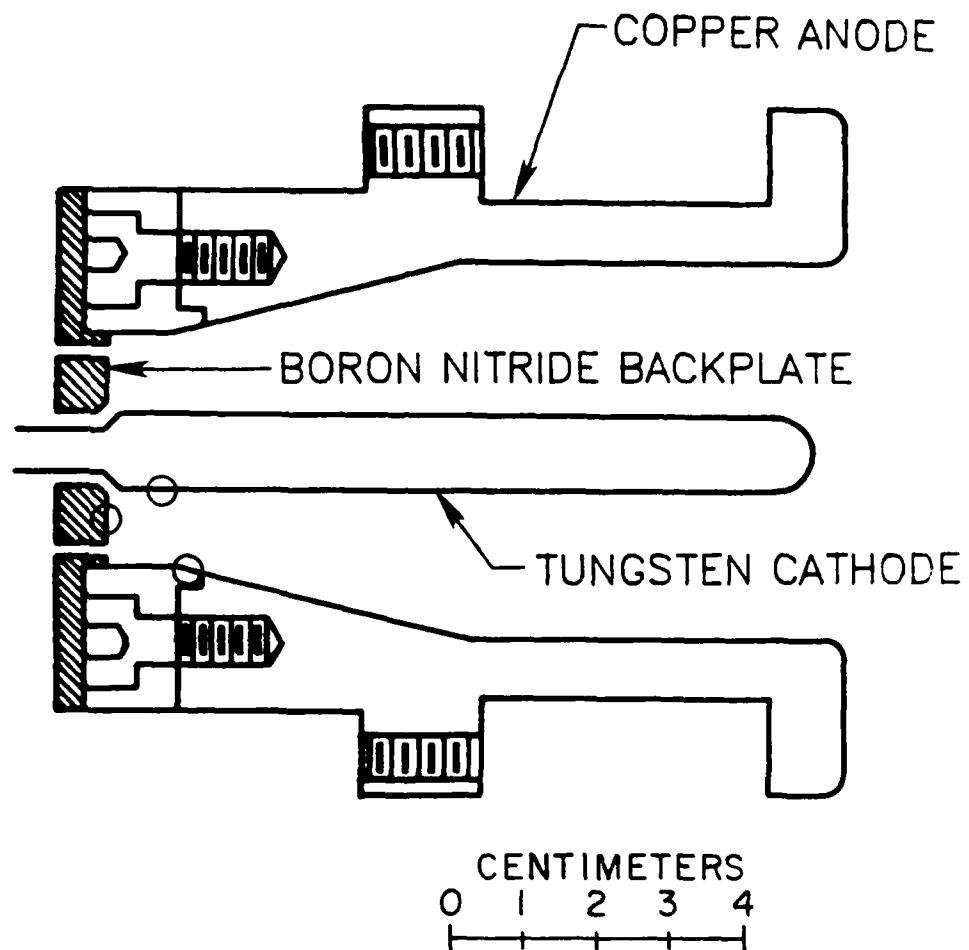


FIGURE 16: CATHODE EROSION VS.  
CHARGE TRANSFER



○ - IRRADIATED POSITIONS

FIGURE 17: HALF-SCALE  
FLARED ANODE THRUSTER

END

DTIC

8-86